https://doi.org/10.5194/egusphere-2024-3941
Preprint. Discussion started: 8 January 2025


# Long-term observations of atmospheric $CO_2$ and $CH_4$ trends and comparison of two measurement systems at Pallas-Sammaltunturi station in Northern Finland

Antti Laitinen[1], Hermanni Aaltonen[1], Christoph Zellweger[2], Aki Tsuruta[1], Tuula Aalto[1], and Juha Hatakka[1]

[1]Finnish Meteorological Institute, Helsinki, Finland
[2]Empa, Swiss Federal Laboratories for Materials Science and Technology, Laboratory for Air Pollution/Environmental Technology, Duebendorf, Switzerland

**Correspondence:** Antti Laitinen (antti.laitinen@fmi.fi)

**Abstract.** Accurate and precise observations of atmospheric greenhouse gas mixing ratios are crucial for understanding the carbon cycle. However, challenges can arise when comparing data between different observation sites, due to different measurement routines and data formats used. To combat these challenges, different research infrastructures have been established in order to harmonize measurement routines and data processing and to make the data from different stations readily available. One of the few stations in the boreal region that observes atmospheric greenhouse gas mixing ratios is the Pallas station, located atop Sammaltunturi fell in Finnish Lapland. The station's location above the arctic circle, far away from large settlements, makes it ideal for measurement of background mixing ratios. The station hosts instrumentation for two different research infrastructures, Integrated Carbon Observation System (ICOS) and Global Atmosphere Watch (GAW), with completely separate gas analyzers, calibration standards and sampling systems. We present the long-term time series of the mixing ratios of $CO_2$ and $CH_4$ and their evolution measured at the station, as well as a long-term comparison of the two instruments during the period when both have been installed. We find that the average difference in the hourly values for $CO_2$ is <0.01 ppm and 0.47 ppb for $CH_4$. The trends and growth rated calculated for both instruments agree well. For a more detailed comparison, the ICOS and GAW systems were simultaneously audited by ICOS Mobile Laboratory and the World Calibration Centre (WCC) of GAW, respectively. The audit results show good agreement between the different systems, with the differences ranging from -0.06 ppm to 0.02 ppm for $CO_2$ and from -0.24 ppb to 0.30 ppb for $CH_4$. No significant dependence on mixing ratio values was found for the differences between the systems. However, for one of the analyzers we found a clear influence of sample drying, especially for $CH_4$. We also compared the long time series with the marine boundary layer reference values in the Northern Hemisphere. For $CO_2$, the values measured at Pallas are on average 1.9 ppm higher than the MBL for Northern Hemisphere, and 54 ppb higher for $CH_4$. The difference is larger during summer for $CO_2$, but not significantly for $CH_4$.

https://doi.org/10.5194/egusphere-2024-3941
Preprint. Discussion started: 8 January 2025


## 1 Introduction

Accurate, long-term observations of the atmospheric greenhouse gas are important for predicting climate change, validating models and satellite observations, and for detecting changes in the composition of the atmosphere. Especially in situ measurements of greenhouse gas mixing ratios are needed for quantifying the long-term trends of the greenhouse gases, as well as annual and interannual variations. They are also crucial for top-down emission estimates using atmospheric inverse models, which aim to optimize fluxes based on measured mixing ratios (Peiro et al. (2022), Crowell et al. (2019)). Together with the bottom-up estimates they give the best estimates for the emissions, crucial for policy makers to understand the sources and sinks of the greenhouse gases. In order to assure consistent measurement quality, WMO has defined compatibility goals that should be reached between different stations and laboratories (WMO, 2024).

One of the few stations conducting atmospheric observations in the boreal region is the station located on top of Sammaltunturi fell in the Pallas-Ylläsjärvi national park in Finland. The Pallas supersite is operated by the Finnish Meteorological Institute (FMI). The station hosts a wide variety of instruments ranging from meteorological measurements to greenhouse gases, aerosols and air quality observations.

The area's initial meteorological observations were conducted near Lake Pallasjärvi, commencing in 1931. Subsequently, in 1991, the measurement station atop Sammaltunturi began its operations. Starting in 1998, the first greenhouse gas measured at Sammaltunturi was carbon dioxide ($CO_2$). Over time, the measurement repertoire expanded to include methane ($CH_4$) in 2004, carbon monoxide (CO) in 2012 and nitrous oxide ($N_2O$) in 2022. In terms of the greenhouse gas measurements, the station is affiliated with two international measurement networks: the Global Atmosphere Watch (GAW) programme of World Meteorological Organization (WMO), and the European-wide Integrated Carbon Observation System (ICOS) (Heiskanen et al., 2022). Within the GAW network, the station is referred to as Pallas-Sammaltunturi (station id: PAL) and it reports data on $CO_2$ and $CH_4$. Meanwhile, under the ICOS network, the station is named Pallas (station id: PAL), and it provides data not only on $CO_2$ and $CH_4$ but also on CO and $N_2O$. This data is also available as GAW data, as ICOS is a contributing network to GAW. More recently, the station has diversified its focus to encompass various features of atmospheric composition. Furthermore, it benefits from the support of multiple measurement sites dedicated to studying atmosphere-ecosystem interactions around the fell. Combined with the different atmosphere-ecosystem interactions stations, the measurement area of Pallas, including Sammaltunturi station, provide a comprehensive insight into the different processes and dynamics of the atmosphere and it's interaction with ecosystems. An overview of the Pallas site is given in Hatakka et al. (2003), and up to date information can be found on the FMI website [1]. While the term Pallas can, in a broader context, refer to the entire supersite, in this paper we use the term Pallas station to refer to the atmosphere station atop Sammaltunturi. The measurement networks ICOS and GAW both aim to achieve high accuracy and comparable observations of the atmospheric composition. While the GAW network focuses on a wider variety of atmospheric components and global coverage, ICOS aims to capture the entire carbon cycle. This includes atmospheric mixing ratio observations of different greenhouse gases, as well as atmosphere-ecosystem interactions

[1] https//en.ilmatieteenlaitos.fi/pallas-atmosphere-ecosystem-supersite, last access: 07.10.2024

https://doi.org/10.5194/egusphere-2024-3941
Preprint. Discussion started: 8 January 2025


through observations of ecosystem fluxes and oceanic carbon. The ICOS Atmospheric Thematic Center (ICOS ATC) oversees the atmospheric measurements of the ICOS network.

To ensure that the station's measurements are compatible with the WMO/GAW goals, they must be compared against other instruments to ensure the differences are within acceptable limits. Such comparisons have been made with travelling cylinders (Zhou et al., 2009) and flask-sampling at the site (Levin et al., 2020). More recently, travelling instruments have been employed at stations to obtain consistent parallel measurements with good results (Hammer et al., 2013; WMO, 2013; Zellweger et al., 2016) . One of the central facilities of the ICOS ATC is the ICOS Mobile Laboratory, is tasked with this exact purpose: auditing the different atmosphere stations by means of parallel measurements and cross-comparisons. The Mobile Lab aims to ensure high quality and accuracy of the ICOS atmospheric measurements. A similar quality management framework exists for the WMO/GAW program. Central Calibration Laboratories (CCLs) maintain and distribute the calibration scales, and World and Regional Calibration Centres (WCCs/RCCs) ensure traceability through independent system and performance audits.

In this paper we give a detailed description of the WMO and ICOS setups used for the atmospheric greenhouse gas measurements at the Pallas station and presents trends, growth rates, seasonal and daily variations of the mixing ratios as well as comparison of the two setups. We focus on $CO_2$ and $CH_4$, which are available from both the ICOS and GAW networks at the Pallas station. In addition, we explore the quality of the Pallas station measurements through comparisons of the two networks as well as the Mobile Laboratory audit and the GAW audit, which was conducted by the WCC for Surface Ozone, CO, $CH_4$ and $CO_2$ (WCC-Empa). We also show how the mixing ratios of $CO_2$ and $CH_4$ at the Pallas station have evolved compared to the global trend in the northern hemisphere, and how well the two separate measurement systems compare over the long term.

## 2 Measurement station

This section presents the details of the Pallas station, location, and instrumentation with a focus on greenhouse gas measurements.

### 2.1 Location

The Pallas station is located in the Pallas-Ylläs national park, in Northern Finland, approximately 860 km from the capital city of Helsinki. The station is on top of a subartic round-topped mountain (Sammaltunturi) (Fig. 1), 566 m above sea level (ASL) and about 100 m above the tree line. It is above the boundary layer most of the time during the winter season and summer nights. On the fell, the vegetation is sparse and mostly consists of low vascular plants, moss and lichen. There are no large cities near the station, with the biggest town, Muonio (approximately 2000 inhabitants), about 20 km west and Kittilä (approximately 6500 inhabitants) about 50 km to south-east from the station. The region around Sammaltunturi has no significant local or regional sources of pollution. The Pallas region lies at the edge of the northern boreal and subartctic climate zones. Mean annual temperature atop the Sammaltunturi (1981-2010) is -1.0 °C, and the mean monthly temperatures vary from -14 °C in January to +14 °C in July. The lowest temperatures are usually measured in February and the highest in July, and the relative humidity is lowest in June and highest in November - January (Fig. 2 (A)). The prevailing wind direction atop the

https://doi.org/10.5194/egusphere-2024-3941
Preprint. Discussion started: 8 January 2025


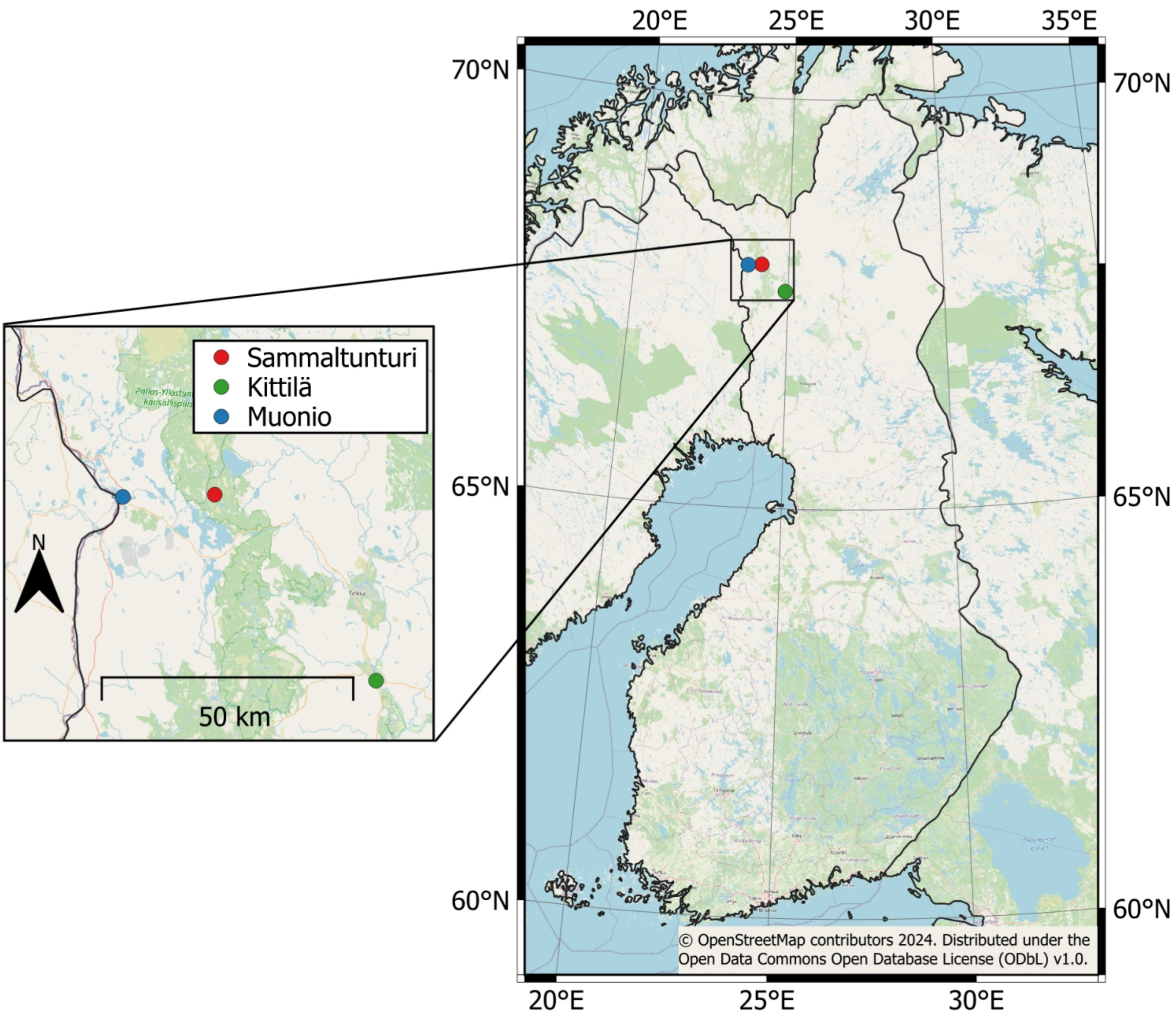


**Figure 1.** Location of Sammaltunturi in Finland. The location of Sammaltunturi in relation to the biggest municipalities Kittilä and Muonio are shown in the inset.

Sammaltunturi is in the West - South axis (Fig. 2 (B)), with very little wind coming in from North. The mean wind speed is 6.9 m/s. The fell of Sammaltunturi is composed of mafic volcanic rock types, which provides a nutritient-rich soil on the fell slopes. The top of the Sammaltunturi fell is treeless and treeline is mostly composed of Norway Spruce. Due to its remote location far away from any local pollution sources, the station measurements are representative for unpolluted background air, and it fulfills the requirements for ICOS Class 1 Mountain Atmosphere Station.

https://doi.org/10.5194/egusphere-2024-3941
Preprint. Discussion started: 8 January 2025


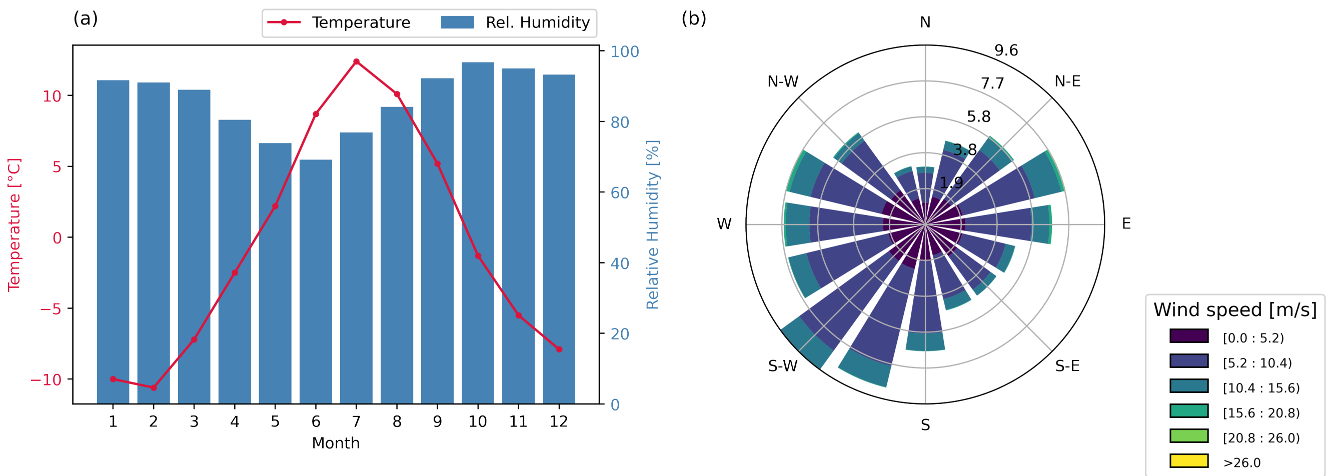


**Figure 2.** Monthly mean temperature and relative humidity (a) and windrose (b) of Sammaltunturi

## 2.2 Instrumentation

During the last 25 years, greenhouse gas instrumentation has undergone substantial improvements in sense of precision, measurement frequency and user-friendliness (Zellweger et al., 2016, 2019). The $CO_2$ measurements at Pallas began with a non-dispersive infrared (NDIR) analyzer in July 1998. For $CH_4$ measurements, a gas-chromatography (GC) based instrument was first used, starting in February 2004. Later, in January 2009, both instruments were replaced by a single cavity ring-down spectroscopy (CRDS) based instrument capable of measuring both species simultaneously. These instruments were producing data for the GAW network, which was later supplemented by a separate CRDS-based instrument producing data for the ICOS network.

Today, the greenhouse gas measurements at Pallas for the GAW and ICOS networks are still completely independent, but both rely on the use of Picarro G2401 and Picarro G5310 (ICOS only) instruments. These commercially available CRDS instruments are capable of measuring mole fractions of $CO_2$ (G2401), $CH_4$ (G2401), CO (G2401 and G5310), $N_2O$ (G5310) and $H_2O$ (G2401 and G5310). To validate the instrument performance, both ICOS instruments have been tested in ICOS Atmosphere thematic centre (ATC) before being set up at the station. The Picarro G5310 was installed in 2022, adding $N_2O$ to the list of continuously measured components and at same time significantly improving CO measurement precision. Although CO is not a greenhouse gas, it is used as a proxy for emissions from anthropogenic sources. Since 2017, when ICOS measurements started at Pallastunturi, ICOS specifications for atmosphere stations have been followed to meet the strict measurement compatibility goals set by the WMO. In Table 1, the network compatibility goals (the maximum bias tolerable when measuring well-mixed background air) and the measurement ranges are presented WMO (2024). All the data presented in this paper, including the data measured during the ICOS Mobile Laboratory and WCC-Empa audits, are reported on the same scale for

https://doi.org/10.5194/egusphere-2024-3941
Preprint. Discussion started: 8 January 2025


| Component | $CO_2$ | $CH_4$ |
|---|---|---|
| Compatibility goal | 0.1 ppm (NH)<br>0.05 ppm (SH) | 2 ppb |
| Extended compatibility goal | 0.2 ppm | 5 ppb |
| Range in unpolluted troposphere | 380 - 450 ppm | 1750 - 2100 ppb |

**Table 1.** WMO Compatibility goals for $CO_2$ and $CH_4$ measurements. For $CO_2$, the goal is separated to northern hemisphere (NH) and southern hemisphere (SH).

each gas. The scale used for $CO_2$ is the WMO $CO_2$ X2019 (Hall et al., 2021) and for $CH_4$ the scale is WMO $CH_4$ X2004A (Dlugokencky et al., 2005).

### 2.2.1 ICOS

Pallas was labelled as an ICOS Class 1 atmosphere station (AS) in 2017. To maintain accuracy, ICOS instruments are automatically calibrated every 360 hours (15 days) and short-term target (STT) cylinder is automatically measured every 15 hours, and also immediately before and after calibration. A long-term target (LTT) cylinder is measured directly after each calibration." As of April 2022, a set of four calibration standards is used (three calibration standards before) in addition to long-term target (LTT) and short-term target (STT) cylinders. The use of these cylinders is in accordance with the ICOS atmosphere station specifications. The calibration and target gases used at the station were prepared by the ICOS Flask and Calibration Laboratory (CAL-FCL). The ICOS sampling inlet is located about five meters from the measurement hut, on the mast 12 meters above the ground level. The sampling inlet collects air samples at a flow of 2 lpm through 1300 Synflex 1/4" tubing with a length of 17 m, which are subsequently partially dried using a Nafion dryer (Perma Pure MD-070-144S-2). The Nafion dryers were installed to the inlets of the ICOS G2401 and ICOS G5310 analyzers in December 2020. Before that time, the air was measured as wet, and corrections to convert to mole fractions in dry air were applied. A Valco SD12MWE valve sequencer is used to switch the sample from ambient air to the calibration and target cylinders (Until April 2022 a solenoid valve sequencer was used). As the dryer is installed directly to the analyzer inlet, the sample drawn from the cylinders is carried through the dryer as well.

The setup of the ICOS instrumentation is illustrated in Fig. 3.

To monitor the quality of the measurements, a long-term and short-term target cylinders are measured to identify any drift in the measurements. The long-term target cylinder measurements for $CO_2$ and $CH_4$ are presented in Fig. 4. The values are given as a bias of the measured value to the assigned cylinder concentration by the CAL-FCL.

In order to make the measured mixing ratios comparable between different stations, the effect of water vapor in the sample must be removed. The resulting dry mole fraction is the comparable physical quantity to report. The water vapor present in the sample air dilutes the mixing ratios of $CO_2$ and $CH_4$ as well as broadening the absorption peaks. The dry mole fractions can be obtained by sufficiently drying the sample, e.g. using cryogenic traps. Another way to account for the water vapor is to correct for the dilution and spectroscopic effects and determine the dry mole fractions computationally. All Picarro instruments are capable of correcting the water vapor effect of the sample and report the dry mole fractions. However, for the analyzers

https://doi.org/10.5194/egusphere-2024-3941
Preprint. Discussion started: 8 January 2025


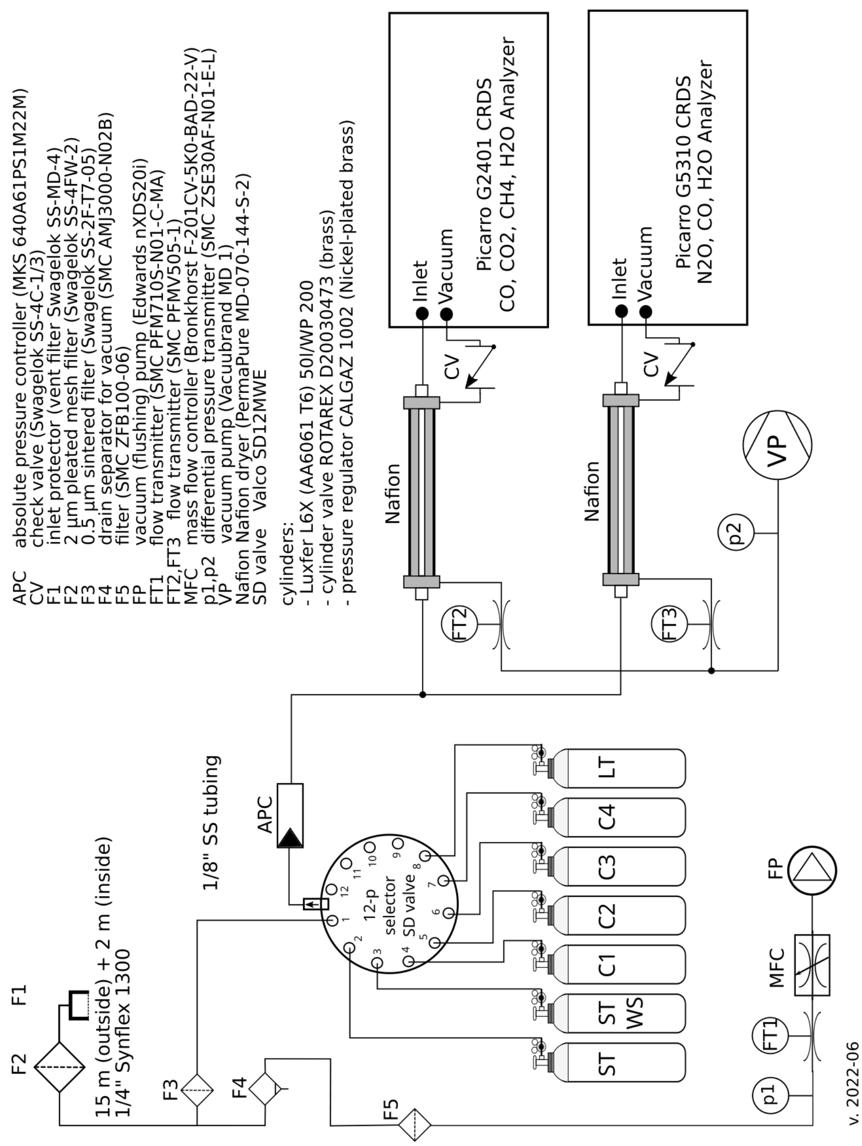


**Figure 3.** Schematic of the ICOS inlet system and manifold of the Pallas station

https://doi.org/10.5194/egusphere-2024-3941
Preprint. Discussion started: 8 January 2025


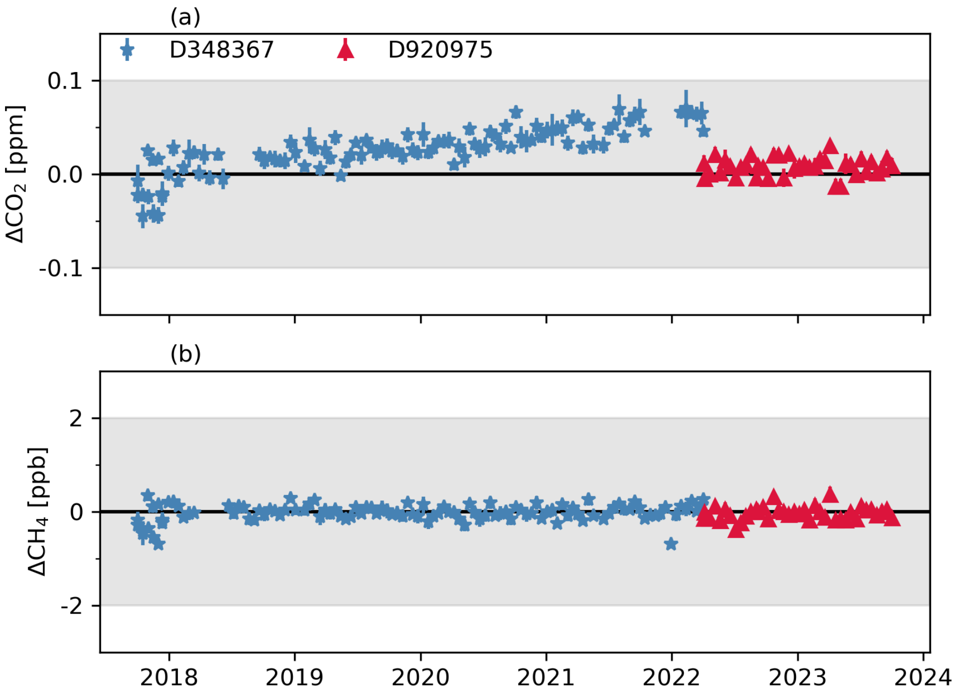


**Figure 4.** Bias of the measured amount fraction to the assigned values of the ICOS target cylinders in $CO_2$ (a) and in $CH_4$ (b). Two different cylinders are marked with different color.

used at ICOS, the correction coefficients are determined for each instrument individually and the correction is applied at the ICOS database. For the GAW analyzer at Pallas, the coefficients are determined by the FMI. The method for calculating the correction functions and correcting the measured mole fractions is presented in Rella et al. (2013). Is it also possible to employ a combination of partly drying the sample, for example with a Nafion dryer, and correcting the data for the remaining water vapor. This approach is used at Pallas for the ICOS system.

To ensure the reliability of the acquired data, a sophisticated two-stage quality control process is implemented. Initially, an automatic quality control algorithm is employed by the ICOS ATC, followed by a manual flagging procedure conducted by the station's principal investigator (PI). The data processing chain implemented the ICOS ATC for $CO_2$ and $CH_4$ is presented in detail in Hazan et al. (2016). All the data measured by the ICOS-related instruments are submitted to the ICOS ATC servers and the processed data is available at the ICOS Carbon portal (Hatakka, 2024c, d).

https://doi.org/10.5194/egusphere-2024-3941
Preprint. Discussion started: 8 January 2025


#### 2.2.2 GAW

The Pallas GAW Picarro is calibrated manually 4-5 times a year. To uphold the accuracy of the measurements between the calibrations, the GAW analyzer automatically measures the short-term target cylinder automatically every 7 hours and 15 minutes and the long-term target cylinder ever 25 hours 15 minutes. The calibration is done by measuring 9 standard cylinders. The GAW analyzer measures humid air and a water vapor correction is applied to the data to calculate the dry mole fractions. The air inlet system of the GAW instrumentation is similar to the ICOS sampling system (Fig. 3), with the difference being in the calibration gases and the absence of the Nafion dryer at the instrument. For the GAW sampling system, the main manifold consists of 60 mm diameter stainless steel tubing which is continuously flushed with a nominal flow rate of 150 $m^3$ $h^{-1}$. The GAW analyzer is connected to the main sampling manifold with a stainless steel tube. The sampling inlet is heated and located on the roof of the measurement building, approximately 7 m above ground level and 3 m above the roof. The calibration standard cylinders used for the GAW analyzers are filled by NOAA, and the STT and LTT cylinders are filled by the FMI. The processing of the GAW data is done by the FMI, and the data is submitted to the GAW database where it is available (Hatakka (2024a, b)).

#### 2.2.3 Flask sampling

In addition to continuous measurements with in-situ gas analyzers, Pallas as a Class 1 ICOS Atmosphere station, is also equipped with an ICOS Flask sampler. The flask sampler contains 24 3 L flasks that are automatically filled on a every three days and sent to CAL-FCL for analysis. The flasks are filled with ambient air, dried to a dew point of about -40 °C, at 1.6 bar overpressure. The main aim of the ICOS Flask samplers is to measure components not measured continuously at the station, such as $SF_6$, $H_2$, stable isotopes of $CO_2$ and $O_2$:$N_2$ ratio. In addition, the flasks are used to control the quality of the continuous measurements by comparing the flask samples to in-situ observations. More detailed description of the ICOS flask sampling strategy is presented by Levin et al. (2020).

### 2.3 Auxiliary measurements

In addition to GHG measurements, meteorological parameters are also measured atop Sammaltunturi. Measured parameters include ambient temperature, relative humidity, pressure, wind speed and wind direction. Air temperature and relative humidity are measured at 7 m height from the ground using a Vaisala HMP155 sensor. The barometric pressure is measured at 2 m height using a Vaisala PTB220 sensor, and the wind speed and direction are measured at 9 m height with a Thies Ultrasonic 2D sensor.

## 3 Methods

The methods used for the time series analysis are presented in Sect. 3.1. The setup and procedure of the ICOS Mobile Laboratory audit is described in Sect.3.2.

https://doi.org/10.5194/egusphere-2024-3941
Preprint. Discussion started: 8 January 2025


### 3.1 Time series

The hourly time series measured with GAW setup was averaged to daily values. A curve was then fitted to the time series using a method developed by Thoning et al. (1989). The curve is fitted to the data in the form

$$f(t) = at^2 + bt + c + c_1 \sin(2\pi t + \vartheta_1) + c_2 \sin(4\pi t + \vartheta_2) + c_3 \sin(6\pi t + \vartheta_3) + c_4 \sin(8\pi t + \vartheta_4) \quad (1)$$

After fitting the function $f(t)$ to the data, the residuals of the fit are calculated. The residuals are then filtered with a low-pass filter to remove any remaining, unwanted oscillations. The filter equation is

$$H(f) = \exp(-\ln(2) \cdot (\frac{f}{f_c})^6) \quad (2)$$

where $f_c$ is the cutoff frequency (in days). Two different cutoff frequencies were used, $f_c$ = 667 for long-term cutoff and $f_c$ = 80 for short-term cutoff. The short-term cutoff is used for smoothing the curve, and the long-term cutoff is used for removing any remaining oscillations that might be present after the fitting. The trend curve, without seasonal oscillations is then calculated by substracting the polynomial part of the Eq. 1 and adding the long-term filtered residuals to that curve. The smoothed curve is calculated by adding the short-term filtered residuals to the Eq. 1.

The yearly growth rate of the time series is calculated from the trend curve by taking the difference of the values of the last and first days of the year. This is approximately equal to the derivative of the trend curve, and gives information on how fast the concentrations are changing. Lastly, the seasonal variation is calculated from the smoothed curve by detrending it, i.e., subtracting the trend part from the smoothed line. The remaining curve shows the seasonal changes in the mixing ratios.

The mixing ratio time series presented in the results section are from the GAW instrumentation, as it is the longest time series available from Pallas. The $CO_2$ time series spans from July 1998 until the end of 2023 and the $CH_4$ time series spans from February 2004 until the end of 2023.

### 3.2 ICOS and GAW audit

As an ICOS station, the Pallas station was audited by the ICOS Mobile Laboratory during spring 2021. The ICOS Mobile Laboratory, operated by the FMI, is designed for visiting the ICOS atmosphere stations, ensuring the quality of their measurement through parallel ambient air comparison measurements as well as cross-comparison of the calibration standard cylinders. This type of additional quality control has been shown to be beneficial in maintaining and improving the quality of the greenhouse gas observations (Hammer et al., 2013; Zellweger et al., 2016).

The Mobile Laboratory is equipped with two Picarro models, G2401 and G5310, and in addition the Ecotech Spectronus FTIR instrument for $CO_2$, $CH_4$, $N_2O$ and CO. For calibration purposes, the Mobile Laboratory carries a set of 6 standard cylinders (hereafter travelling cylinders standards, TC's) filled by the ICOS FCL. Three of the cylinders are used for calibration purposes, two are used as the short-term and long-term targets cylinders for G2401 and G5310 and one is used as the target for the FTIR instrument. In order to account for a potential drift of the travelling standards, they are regularly compared to laboratory standards between the audit campaigns. The Mobile Laboratory is also equipped with a freeze dryer (model

https://doi.org/10.5194/egusphere-2024-3941
Preprint. Discussion started: 8 January 2025


ICOS) for drying the sample air, as well as a water-bench for evaluating the humidity correction coefficient of the stations' G2301/G2401 instruments.

The Mobile Laboratory audit consists of two visits to the station, one at the beginning and one at the end of the approximately six weeks long parallel measurement period. During this period, all the Mobile Laboratory instruments are sampling ambient air in parallel with the station instruments, through a dedicated spare sampling line. During this time the Mobile Laboratory instruments are calibrated automatically every 10 days, the short-term target cylinder is measured every 8 hours and the long-term target cylinder every 10 days. The station instrument is operating according to its normal operation schedule.

During the two visits, the station's calibration cylinders and the TSs are cross-compared to trace any possible issues related to the cylinders or the instrument. The Mobile Laboratory also performs a water vapor test on the station's analyzer in order to assess the validity of the internal water vapor correction coefficient. As all of the measurements and tests are performed during both visits, any possible drift in the cylinder concentrations, instrument performance or the water vapor correction coefficients can be tracked.

At the same time as the audit of the ICOS mobile laboratory, which focused on the ICOS system, an audit of the GAW system was carried out by WCC-Empa. The GAW measurements at Pallas have been audited three times in the last 2 decades: in 2007, in 2012 and most recently in 2021 (latest report: (WMO, 2022)). The WCC instrumentation consists of a single Picarro G2401 for $CO_2$, $CH_4$ and CO measurements. For $CO_2$ and $CH_4$, the calibration is performed with a single standard. The instrument was also calibrated with $CO_2$ and $CH_4$ free air (zero) prior to field use. To account for drift, an additional working standard is used, and the stability of the calibration is checked using a target tank. For CO, all three standards were used to calibrate the instrument. The sample air was dried using a Nafion dryer (Permapure, Model MD-070-48S-4), and the WCC-Empa Picarro was calibrated every 1445 minutes. The WCC-Empa analyzer sampled air from a location close to the ICOS Picarro and the ICOS Mobile Laboratory inlets using a 1/4" Synflex-1300 line flushed by an external pump at 3 l/min. The joint audit period ran from 05.03.2021 until 19.04.2021.

### 3.3 Data comparison

The data of the ICOS and GAW instruments were compared at both hourly and daily resolutions, starting in September 2017, when the ICOS instrument was installed at Pallas. In order to focus on the regional signal, the data was filtered based on the wind speed and the standard deviation of the hourly measurements. The lower limit for the wind speed is 3 m/s during summertime (June-August) and 4 m/s during wintertime, and the standard deviation less than 0.5 ppm ($CO_2$) or 3 ppb ($CH_4$). Based on this criterion, approximately 31 % of the $CO_2$ and 23 % of $CH_4$ hourly data were discarded.

In addition, in order to remove any hourly means with possible biased sampling (i.e. if a calibration sequence starts in the middle of the hour, causing the hourly mean to represent only part of the hour), only hours with 60 minutes of measurements from both instruments were considered.

To quantify the effect of the different systems on the fitted trend lines and growth rates, a curve according to Eq. 1 was fitted to the time series from both systems for the time period of concurrent measurements. The mean difference between the trend

https://doi.org/10.5194/egusphere-2024-3941
Preprint. Discussion started: 8 January 2025


lines is calculated as well as the confidence intervals. From the trend lines, the annual growth rate was calculated for both systems and their differences are reported.

Often the convention is to calculate the daily averages from the afternoon hours in order to maximise the boundary layer mixing (Resovsky et al., 2021). We also calculated the daily means using this method and compared the differences with the data filtered by wind speed and hourly standard deviation. The exact hours chosen may vary from station to station, here the hours 12:00 - 17:00 (EET) are used.

## 4 Results and discussion

The results of the time series analysis are presented in this section. For each measured component a time series is presented along with a fitted curve to the data and a long-term time series without seasonal oscillations. In addition to the mixing ratios, a growth rate for each component is calculated according to method described Sect. 3. Average diurnal and seasonal cycles are also presented.

### 4.1 $CO_2$

The observed daily $CO_2$ mixing ratios from the GAW measurements at PAL as well as the Northern Hemisphere mean marine boundary layer (MBL) from NOAA (Lan et al., 2024a) are presented in Fig. 5 (top) along with the annual growth rates for GAW observations and MBL data (bottom).

Consistent with the global trend, the $CO_2$ levels have risen steadily at a rate of approximately 2 ppm/year from 373 ppm (1999 mean) to 423 ppm (2023 mean).

Likely due to the location, the background mixing ratios measured at Pallas are, in general, higher than the average in the Northern Hemisphere. The mean difference in the daily average is 1.9 ppm (95% CI: -8.0 ppm-11.8 ppm). This difference is significantly higher during the cold season (approximately September-April) with a mean difference of 4.10 ppm (95% CI: -3.1 ppm-12.8 ppm) than during the warm season (approximately May - August), when the mean difference is -2.7 ppm on average (95% CI: -9.9 ppm-3.0 ppm).

The average growth rate of about 2 ppm/year at Pallas is comparable to the globally observed changes in $CO_2$ (Fig. 5).

Measured $CO_2$ mixing ratios at Pallas station are representative for a large area due to its remote location, and no significant anthropogenic sources are present near the station. $CO_2$ sinks at Pallas are mostly vegetation, and the effect can be seen in the seasonal cycle (7, bottom). The seasonal cycle is well defined, the yearly maximum is, on average, on day 37 (beginning of February) and the minimum on day 220 (beginning of August) (calculated as the annual minima and maxima of the smoothed curve). During the vegetation period (approximately May-September) a diurnal cycle is also visible (7, top) with a mean amplitude of 4.2 ppm, indicating the influence of local vegetation. During the winter months no diurnal variation is visible.

The hourly and daily the biases between the ICOS and GAW measurement systems are presented in Fig. 6.

https://doi.org/10.5194/egusphere-2024-3941
Preprint. Discussion started: 8 January 2025


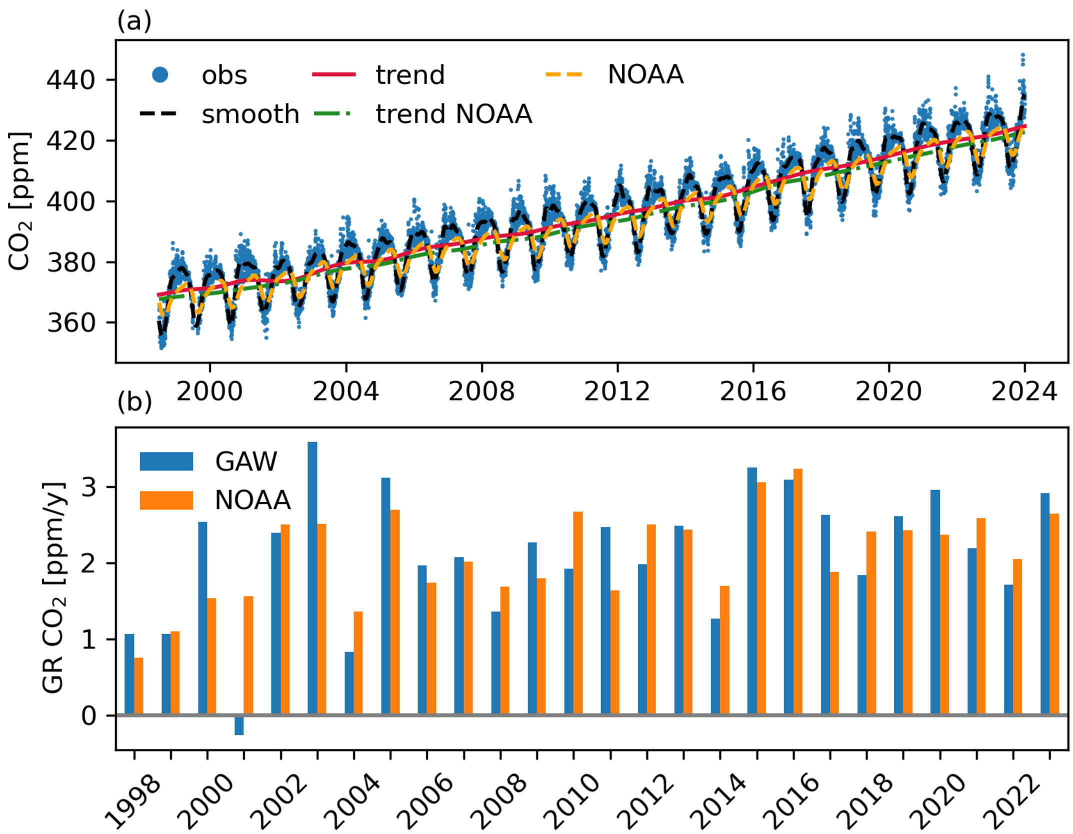


**Figure 5.** Time series of $CO_2$ (a). The blue dots indicate the daily observed values from the GAW instrument, the red line the trend value derived from the GAW observations and the black dashed line the smoothed line from the GAW observations. The yellow dashed line indicates the MBL data and the green dotted line the trend derived from the MBL. Yearly growth rates of $CO_2$ for GAW measurements (blue) and the NOAA MBL data (orange) (b).

https://doi.org/10.5194/egusphere-2024-3941
Preprint. Discussion started: 8 January 2025


The differences of the instruments fit well within the WMO/GAW compatibility goals: for daily measurements, 94.7 % of the days are within the assigned limits, and for hourly measurements, 93.3%. The mean difference is <0.01 ppm (95% CI: -0.07-0.10 ppm) for the daily means and <0.01 ppm (95% CI: -0.10-0.13 ppm) for the hourly means.

With the addition of the Nafion dryer to the ICOS analyzer inlet at the end of 2020, the differences between the two instruments were slightly changed: Before the Nafion was added, the average hourly difference was 0.01 ppm (CI: -0.10-0.13 ppm) and the average daily difference was 0.02 ppm (CI: -0.07-0.11 ppm). After the addition of the Nafion dryer, the hourly differences was -0.02 ppm (CI: -0.10-0.12 ppm) and the daily difference was -0.02 ppm (CI: -0.07-0.10 ppm). Thus, the Nafion dryer appears to slightly increase the absolute difference between the measurements, but at the same time it reduces the spread of the differences. Before the the addition of the Nafion dryer, 91.9% of the hourly data and 94.1% of the daily data fit within the WMO/GAW limits. After the addition of the Nafion 94.8% of the hourly data and 95.3% of the daily data fit within the limits. Overall, the drying the sample air with a Nafion dryer seems to be beneficial for the $CO_2$ measurements. The agreement of the trend lines fitted for both time series was excellent, with the mean difference being 0.02 ppm. Calculating the yearly GRs from both trend lines also agree well with mean difference of 0.01 ppm/year.

When the data is filtered to include afternoon hours only, the differences between the two systems is 0.01 ppm ppm (95% CI: -0.10-0.09 ppm), which is almost identical to the filtering based on wind speed and hourly standard deviation.

Results of the combined ICOS and GAW audit are presented in Fig. 8. During the audit period, both the ICOS Mobile Laboratory analyzer and the WCC-Empa travelling analyzer were sampling from a dedicated sampling line and inlet, located next to the inlet of the local ICOS system. As the ICOS inlet is in a slightly different location than the GAW inlet, the measured time series can be at times inconsistent in case of local emissions episodes. In order to provide comprehensive overview of the differences in the measured time series, no distinction has been made between regional and local signals, in contrast to the long-term comparison between the ICOS and GAW systems.

The summarized results of each $CO_2$ comparison is presented in Table 2. The differences between the instrumentation are consistent in time, and are mostly within the WMO/GAW compatibility goals. The best agreement is found between the ICOS Mobile Laboratory and the ICOS system, but also all the other comparisons fit within the compatibility goals. The largest spread in the confidence intervals are found between the GAW and Mobile Laboratory and WCC-Empa and the ICOS Mobile Laboratory measurements. The former is probably due to the different inlet locations. For the latter, it is difficult to find a definitive reason, but the different flow rates in the instruments could play a role. In general the spread of the confidence intervals between the different comparisons is consistent, and with the exception of the GAW comparison with the ICOS Mobile Laboratory, all comparisons fall within the compatibility goals within 95% CI. All the measured analyzer pairs had linear relationship and no significant dependency on the mixing ratio was evident on the agreement between the analyzers (Fig 9).

A study by Hammer et al. (2013) compared a fourier transform infrared (FTIR) based travelling instrument to a reference instrument at Heidelberg (HEI) as well as to local instruments at two field stations, Cabauw (CBW) and Houdelaincourt (OPE) on 3-minute aggregated data. Their results show median differences between the travelling instrument and the local instrument being -0.02 ppm at HEI, -0.21 ppm at CBW and 0.13 ppm at OPE. Similarly, a study by Vardag et al. (2014) compared similar

https://doi.org/10.5194/egusphere-2024-3941
Preprint. Discussion started: 8 January 2025


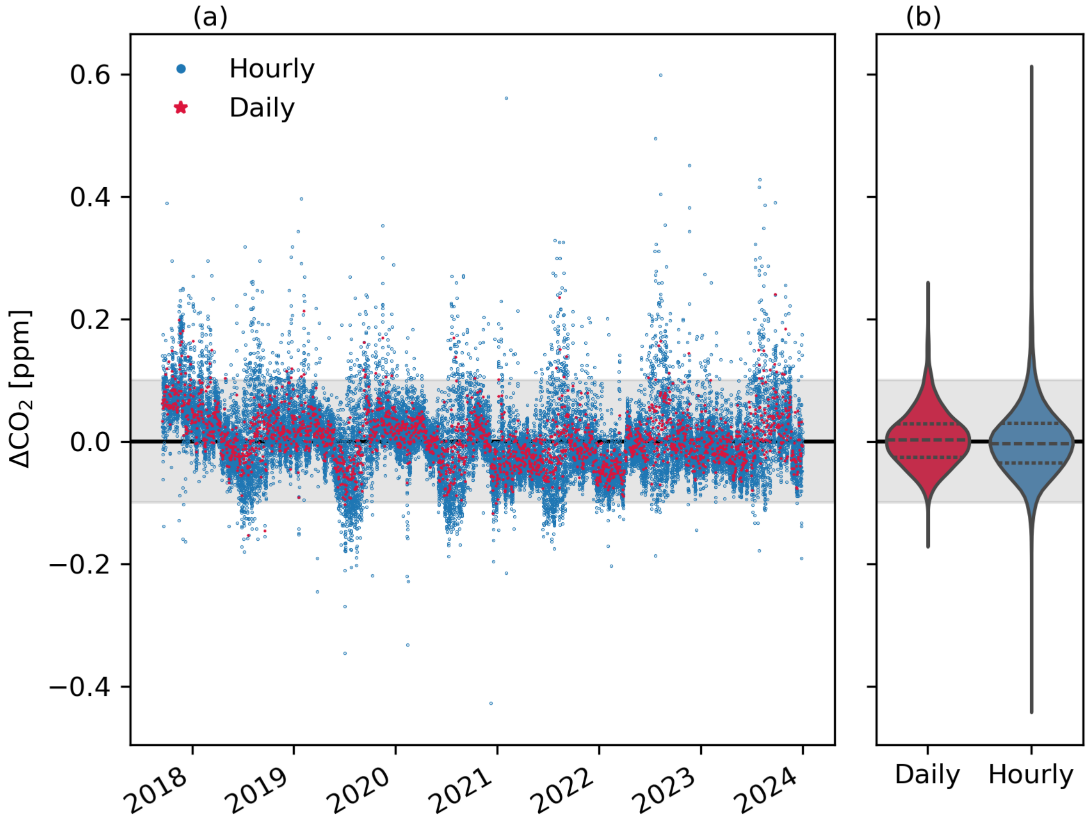


**Figure 6.** Panel (a): Time series of the differences between the ICOS and GAW instruments for $CO_2$. The blue dots indicate the hourly mean values and red dots the daily mean values. Panel (b): distribution of the data points. The gray shaded areas indicate the WMO/GAW compatilibity goals.

FTIR instrument at HEI and at a field station in Mace Head (MHD); they found median differences of 0.03 ppm and 0.04 ppm at HEI (before and after the MHD campaign) and 0.14 ppm at MHD. Our results thus show a rather good agreement, comparable even with the results at Heidelberg where the TI was compared against a reference instrument. However, our results compare hourly means while Hammer et al. (2013) and Vardag et al. (2014) compare 3-minute means.

## 4.2 $CH_4$

The measured daily $CH_4$ mixing ratios as well as the mean marine boundary layer means in the Northern Hemisphere (NOAA $CH_4$ MBL, Lan et al. (2024b)) are presented in Fig. 10.

https://doi.org/10.5194/egusphere-2024-3941
Preprint. Discussion started: 8 January 2025


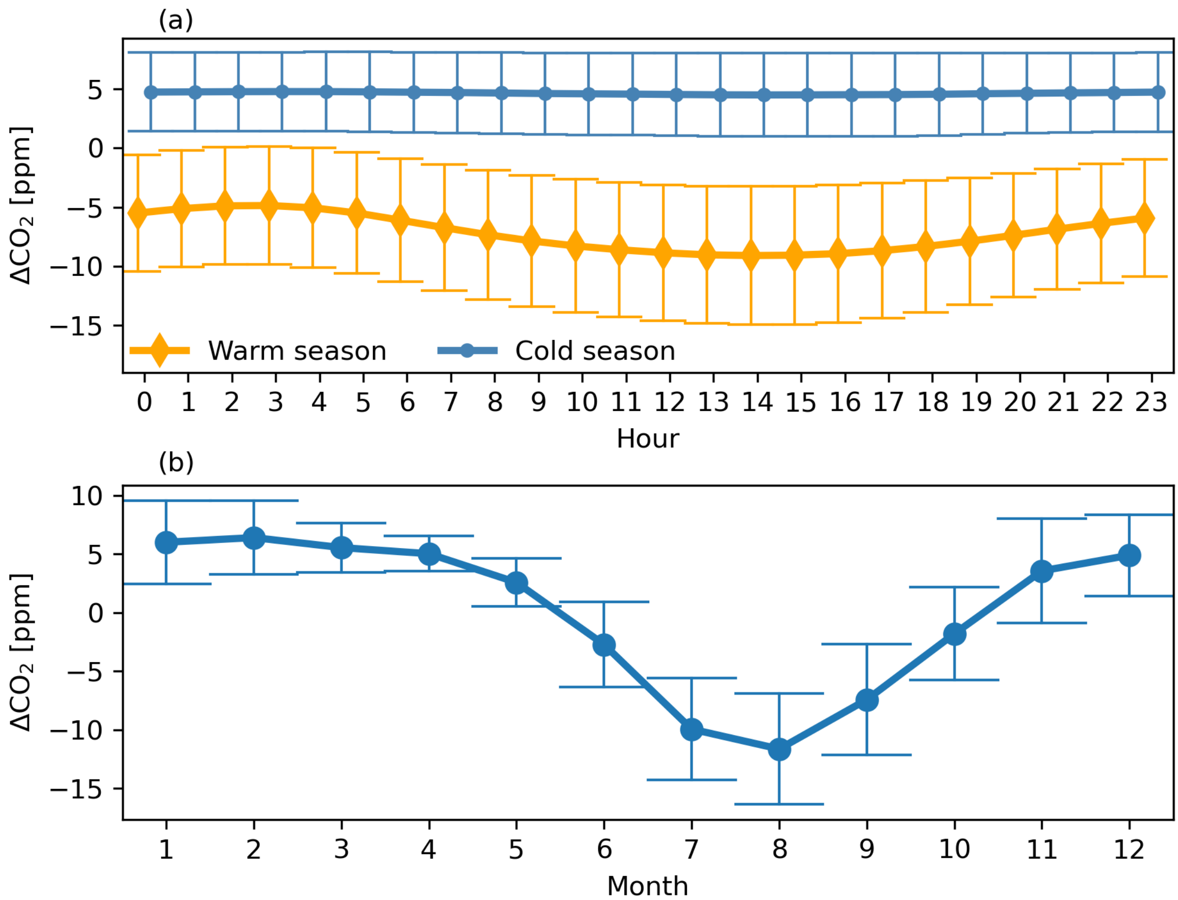


**Figure 7.** Average diurnal cycle of during the warm and cold seasons (deviation from the trend line) for $CO_2$ (a) and the average seasonal variation of $CO_2$ (deviation from the trend line) (b)

As for $CO_2$, the $CH_4$ mixing ratios measured at Pallas are higher than the average for the Northern Hemisphere because the station is located at high latitude. At Pallas the mixing ratios have increased from 1865 ppb in 2004 to 2023 ppb in 2023, while in the Northern Hemisphere on average the mixing ratios have increased from 1819 ppb in 2004 to 1969 ppb in 2023. On average the mixing ratios at Pallas are 54 ppb higher than on the average in the Northern Hemisphere. There is no significant difference between the cold and warm seasons as in $CO_2$, indicating little influence of the local vegetation to $CH_4$. A definite seasonal and diurnal cycles during the warm period are also visible in $CH_4$ timeseries (Fig 11. Amplitude of the diurnal cycle during the warm period is approximately 6.5 ppb and the amplitude of the seasonal variation 35.7 ppb. The seasonal cycle has the highest values usually in January, and a second peak exists in September. Lowest values for the seasonal cycle are usually in June.

https://doi.org/10.5194/egusphere-2024-3941
Preprint. Discussion started: 8 January 2025


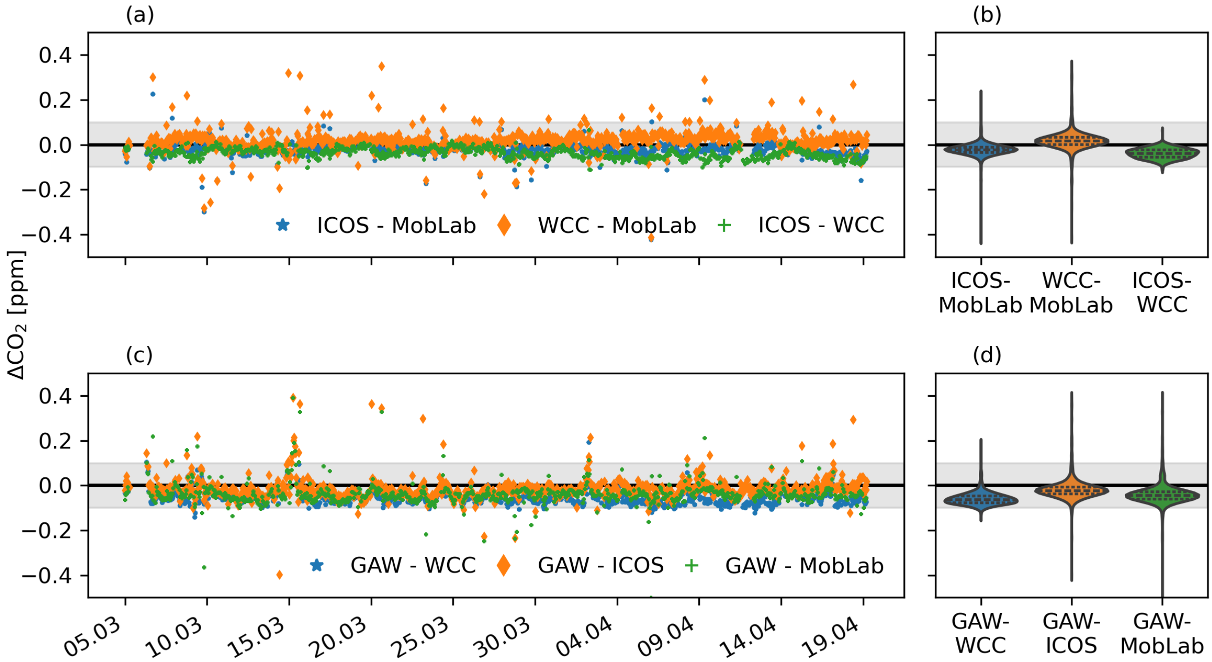


**Figure 8.** Time series of the differences for different comparison pairs (a and c), and their associated distributions (b and d) for $CO_2$.

| | Mean (ppm) | 95% CI (ppm) | CI range (ppm) | Slope | Intercept |
|---|---|---|---|---|---|
| Full period | | | | | |
| ICOS - GAW | <0.01 | -0.10-0.13 | 0.23 | 0.999 | 0.32 |
| Audit period | | | | | |
| ICOS-Mobile Lab | -0.02 | -0.07-0.02 | 0.09 | 1.000 | 0.19 |
| GAW-MobLab | -0.04 | -0.10-0.07 | 0.17 | 1.002 | -0.69 |
| WCC-MobLab | 0.02 | -0.06-0.11 | 0.17 | 0.998 | 0.97 |
| ICOS-WCC | -0.04 | -0.08-0.00 | 0.08 | 1.001 | -6.7 |
| GAW-WCC | -0.06 | -0.10-0.01 | 0.11 | 1.002 | -0.84 |
| ICOS-GAW | -0.02 | -0.08-0.10 | 0.18 | 0.998 | 0.97 |

**Table 2.** Results of the cross-comparisons of different analyzers on hourly mean data over the full period and during the audit period for $CO_2$. For the full period, the data is filtered for wind speed, however during the audit period no wind speed filtering is applied.

https://doi.org/10.5194/egusphere-2024-3941
Preprint. Discussion started: 8 January 2025


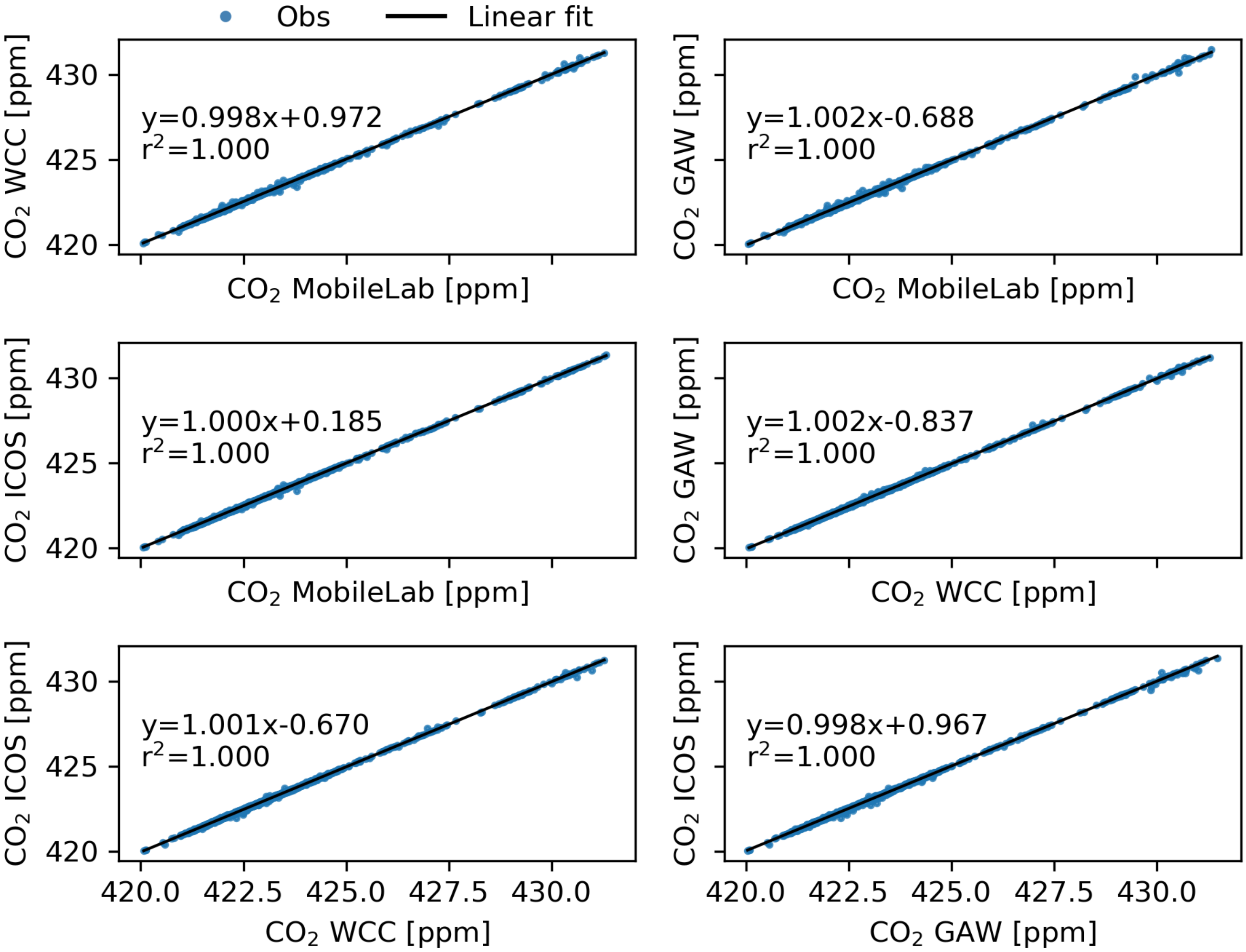


**Figure 9.** Scatterplots and linear regressions fitted to each measurement pair for $CO_2$.

https://doi.org/10.5194/egusphere-2024-3941
Preprint. Discussion started: 8 January 2025


Major $CH_4$ sources in the Arctic that influence the mixing ratios at Pallas are anthropogenic sources and wetlands followed by freshwater systems. Of the Arctic sources, during wintertime anthropogenic emissions contribute up to 56% and during summertime the wetland emissions contribute up to 70% and freshwater systems up to 26% (Thonat et al., 2017). However, major contribution is still from emissions originating outside of the Arctic area.

The $CH_4$ concentrations have been increasing rapidly after 2019, and the growth rate peaked in 2020. The increase in the methane in 2007-2017 can likely be attributed to the increased emission from wetlands (Nisbet et al., 2016, 2019). The more recent increase in 2020 could be attributed to the increased wetland or anthropogenic emissions locally (Yuan et al. (2024); Tenkanen et al. (2024); Ward et al. (2024)) as well as decrease in atmospheric sinks (Peng et al., 2022; Stevenson et al., 2022; Qu et al., 2022; Feng et al., 2023). However, the increase measured at Pallas is significantly higher than on the average in the northern hemisphere, indicating a strong increase of local and regional emissions.

The hourly and daily biases between the ICOS and GAW analyzers for $CH_4$ are presented in Fig. 12.

As for $CO_2$, the measurements of the ICOS and GAW instruments for $CH_4$ agree very well. The mean difference for the hourly measurements is 0.47 ppb (95% CI: -0.40-1.53 ppb) and for daily measurements the mean is also 0.47 ppb (95% CI: -0.36-1.39 ppb).

The differences show a seasonal variation with higher differences in the winter compared to summer until the end of 2020, after which the variation is significantly reduced, indicating the effect of a Nafion dryer installed to the inlet of the ICOS analyzer. This suggests that the seasonal variation is driven by varying humidity from summer to winter. As the drying process eliminates most of the moisture from the sample, the variation is reduced. However, the strong variation due to the sample humidity seems to be solely caused by the ICOS analyzer, since the GAW analyzer always measures the sample air wet. The discrepancy could also be caused by better performance of water vapor correction of the GAW analyzer compared to the ICOS analyzer. Before the installation of the Nafion dryer the mean hourly difference is 0.77 ppb (95% CI: -0.34-1.69 ppb) and the mean daily difference is 0.76 ppb (95% CI: -0.27-1.54); after the Nafion installation the mean hourly difference drops to 0.14 ppb (95% CI: -0.53-0.90 ppb) and the daily mean difference drops to 0.16 ppb (95% CI: -0.38-0.74 ppb). Before the Nafion installation, 99% of the measured hours and 99.7% of the measured days were within the WMO compatibility goals; after installation 99.9% of the hours and virtually all (100%) of the days were within limits.

The agreement of the two fitted trend lines was good, with the mean difference being 0.3 ppb. Calculating the yearly GRs from both trend lines also agree well with mean difference of 0.1 ppb/year.

When the data is filtered to include afternoon hours only, the differences between the two systems is 0.46 ppb (95% CI: -0.43-1.52 ppb), which is slightly higher but not significantly different from the filtering based on wind speed and hourly standard deviation.

The results of the combined ICOS and GAW audit for $CH_4$ are presented in Fig. 13. As for the $CO_2$ comparison, the measurements are on an hourly resolution. The ICOS Mobile Laboratory hourly data is calculated from the minute data matching the ICOS data (i.e., minutes not measured by the local ICOS analyzer due to calibration etc. are not included in the Mobile Laboratory hourly means), and the WCC-Empa hourly data is similarly matched to the GAW Picarro data.

https://doi.org/10.5194/egusphere-2024-3941
Preprint. Discussion started: 8 January 2025


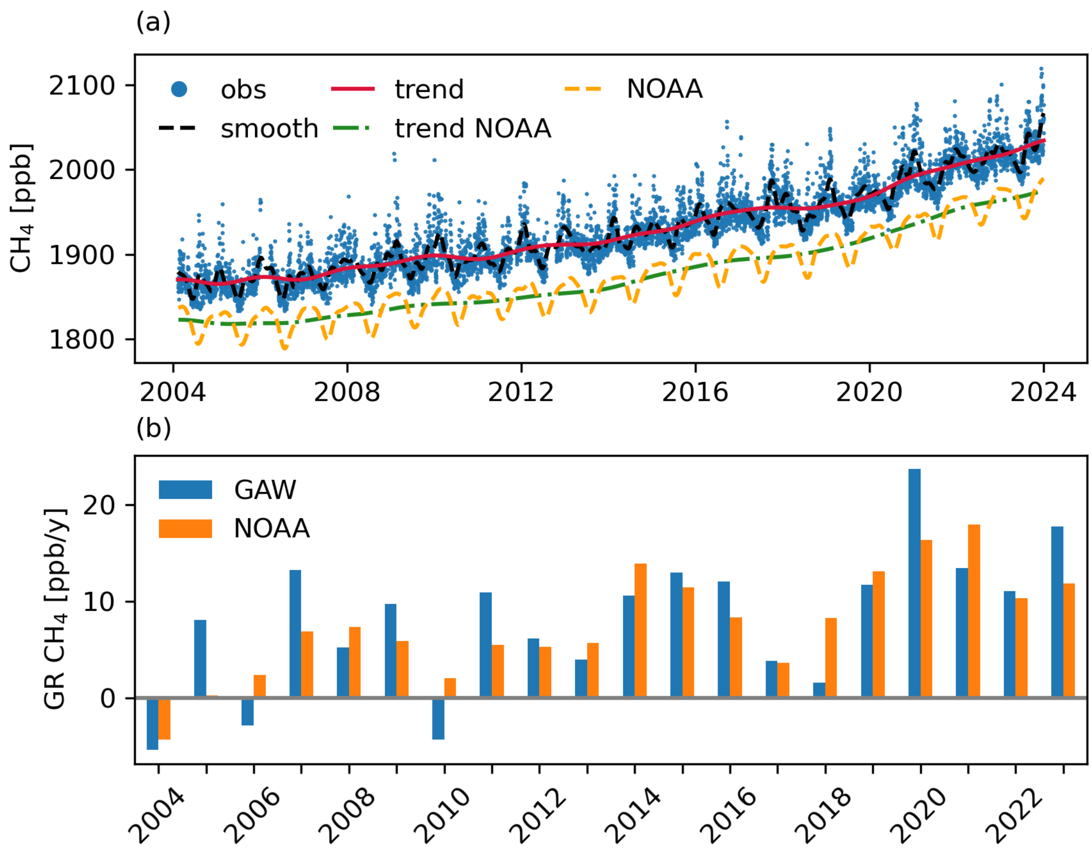


**Figure 10.** Panel (a): Time series of $CH_4$. The blue dots indicate the daily observed values from the GAW instrument, the red line the trend value derived from the GAW observations and the black dashed line the smoothed line from the GAW observations. The yellow dashed line indicates the MBL data and the green dotted line the trend derived from the MBL. Panel (b): The yearly growth rates of $CH_4$ for GAW measurements (blue) and the NOAA MBL (orange).

https://doi.org/10.5194/egusphere-2024-3941
Preprint. Discussion started: 8 January 2025


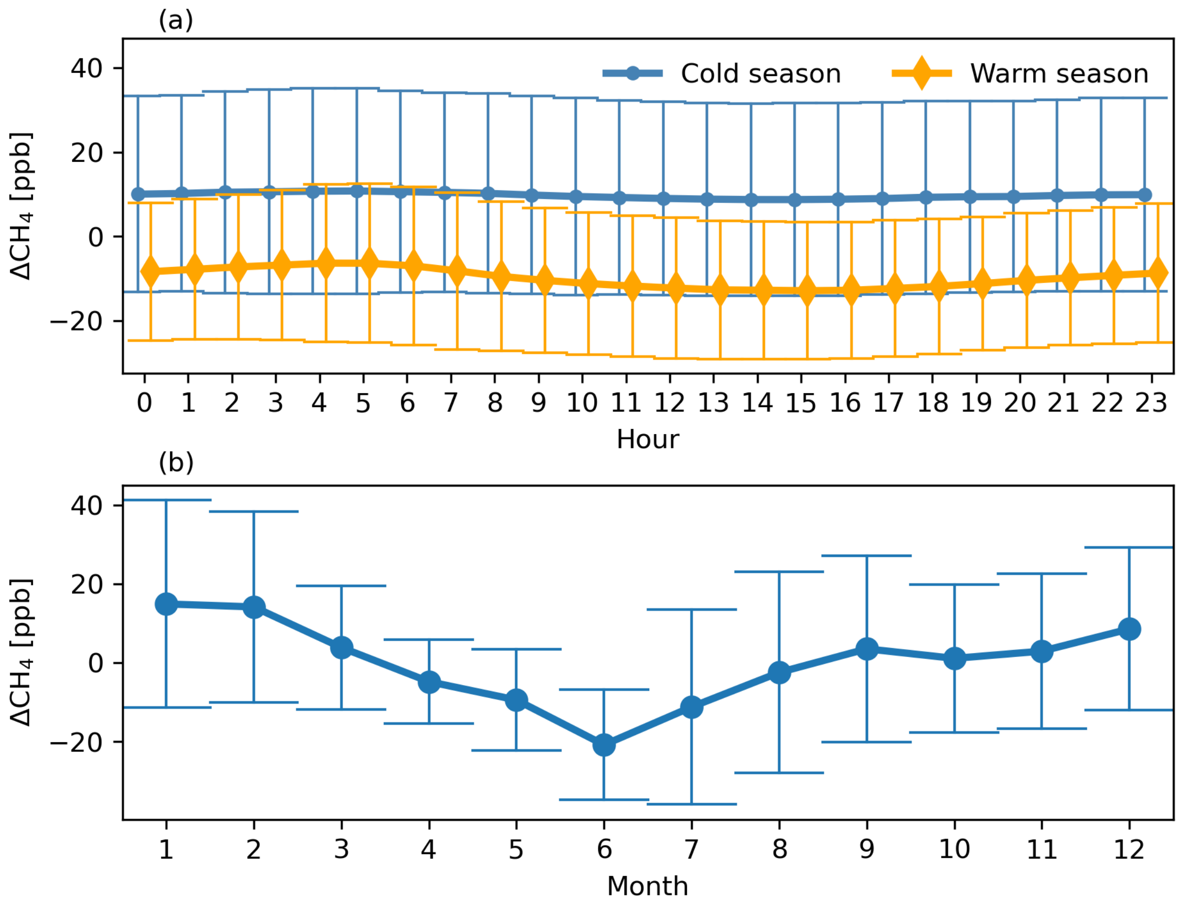


**Figure 11.** Average diurnal cycle of the during the warm and cold seasons for $CH_4$ (a) and average seasonal variation of $CH_4$ (b). Both are calculate from de-trended timeseries.

Results of the audit are summarized in Table 3. The mean difference of each comparison is well within the WMO/GAW compatibility goals. The largest differences are observed between GAW and WCC and between GAW and Mobile Laboratory. It seems that the GAW analyzer is measuring slightly higher values compared to the other analyzers. This could be an issue of the sampling line or inlet, as the GAW analyzer is the only instrument sampling from a different location than the rest of the instruments. Furthermore, all the instruments are calibrated using a separate set of calibration standards, which could cause differences in the calibrated values. However, despite these differences in the setup, sampling and calibration, the differences between the instruments remain small. The spreads of the differences are also consistent between the instruments as well, and all the 95% intervals are within the compatibility goals. The largest spreads are found between the GAW and the ICOS Mobile Laboratory and between WCC and ICOS Mobile Laboratory instruments. As for $CO_2$, no significant dependency on the mixing ratio was found in the agreement between two analyzers for each pair (Fig. 14)

https://doi.org/10.5194/egusphere-2024-3941
Preprint. Discussion started: 8 January 2025


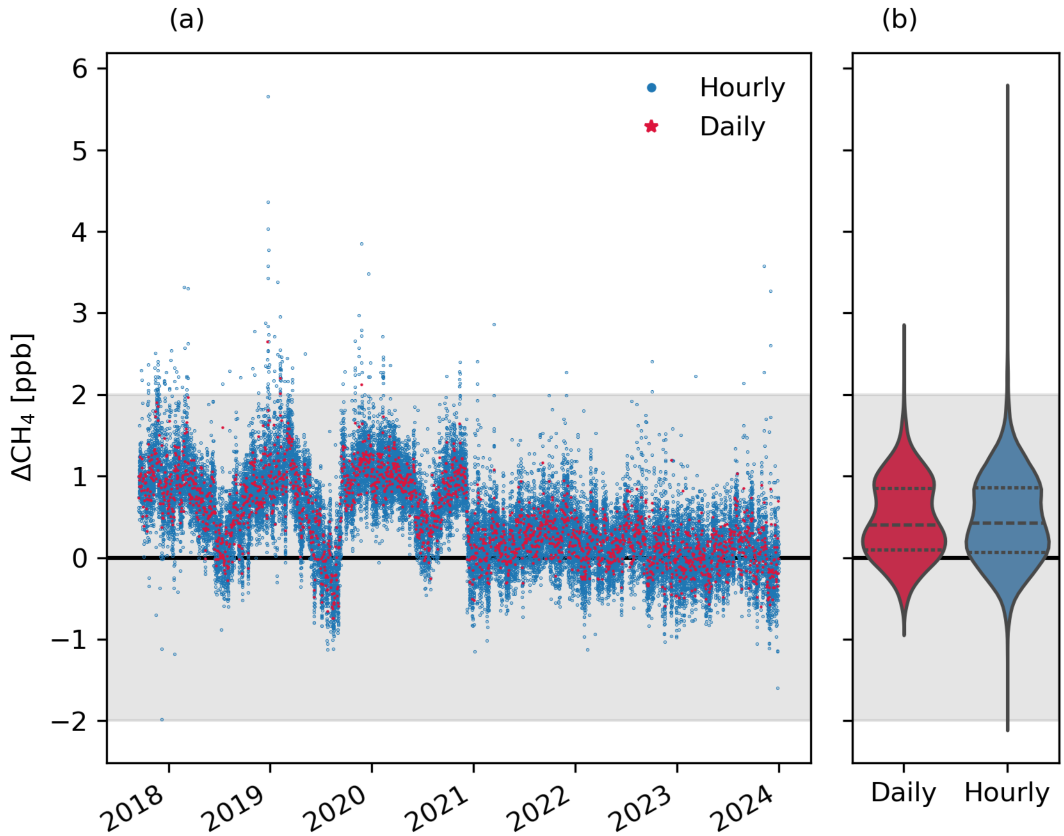


**Figure 12.** Panel (a): Differences between the ICOS and GAW instruments for $CH_4$. The blue dots indicate the hourly mean values and red dots the daily mean values. Positive/negative values indicates $CH_4$ measured by the ICOS instruments are higher/lower than those from GAW. Panel (b): distribution of the data points . The gray shaded areas indicate the WMO/GAW compatilibity goals

As for $CO_2$, Hammer et al. (2013) compared $CH_4$ measurements as well. For $CH_4$ the results show median bias of -0.3 ppb against the reference instrument at HEI, 0.41 ppb at CBW and 0.44 ppb at OPE. Our comparisons for $CH_4$ show similar results between GAW-MobileLab, GAW-WCC and ICOS-GAW comparisons. The other study by Vardag et al. (2014) found median differences of -0.04 ppb and 0.12 ppb at MHD, when comparing the travelling instrument to the two local instruments at MHD. At HEI the median difference of $CH_4$ was -0.25 ppb before the campaign at MHD and -0.24 ppb after.

## 5 Summary

In this article, we present the measurements of $CO_2$ and $CH_4$ at the Pallas station (Sammaltunturi) located in the Pallas-Yllästunturi national park in Finnish Lapland, as well as a comparison of the two measurement setups at the station. A compre-

https://doi.org/10.5194/egusphere-2024-3941
Preprint. Discussion started: 8 January 2025


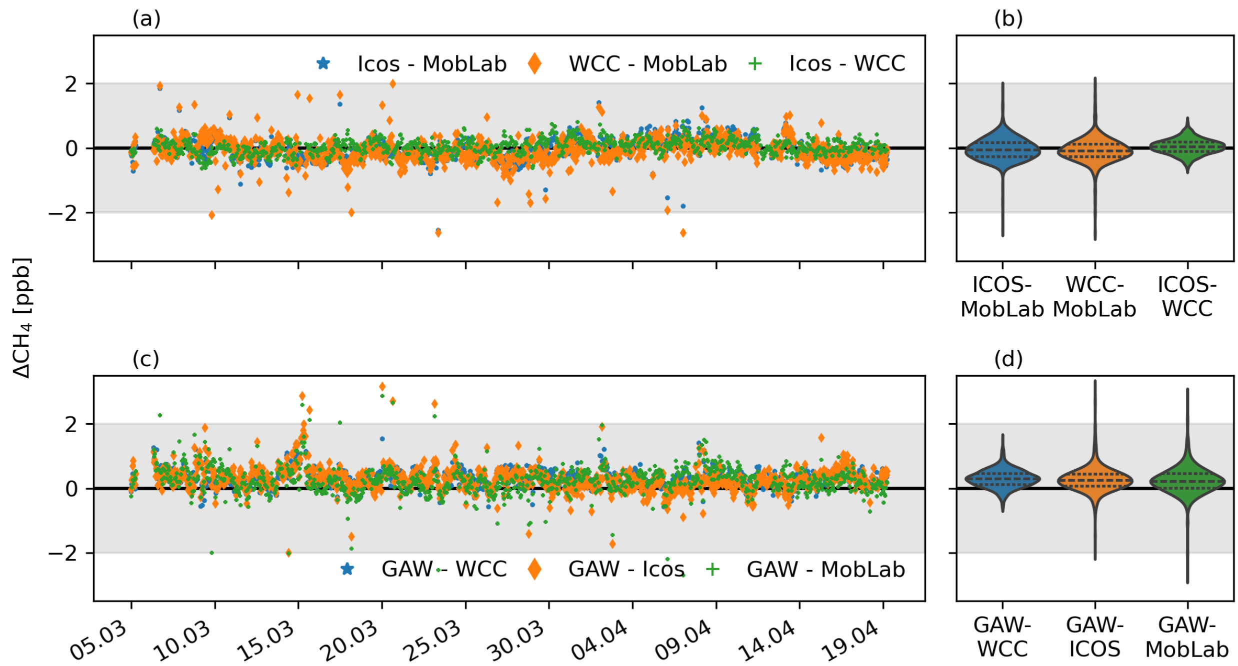


**Figure 13.** Time series of the differences for different comparison pairs (a and c), and their associated distributions (b and d) for $CH_4$.

| | Mean (ppb) | 95% CI (ppb) | CI range (ppb) | Slope | Intercept |
|---|---|---|---|---|---|
| Full period | | | | | |
| ICOS - GAW | 0.55 | -0.4-1.16 | 1.56 | 0.994 | 11.62 |
| Audit period | | | | | |
| ICOS-Mobile Lab | -0.04 | -0.59-0.62 | 1.20 | 0.999 | 2.25 |
| GAW-MobLab | -0.24 | -0.44-1.16 | 1.60 | 1.002 | -4.06 |
| WCC-MobLab | -0.08 | -0.76-0.58 | 1.34 | 1.000 | -0.66 |
| ICOS-WCC | 0.05 | -0.44-0.54 | 0.98 | 0.999 | 2.89 |
| GAW-WCC | 0.30 | -0.25-0.85 | 0.98 | 1.001 | -1.26 |
| ICOS-GAW | 0.27 | -0.38-1.02 | 1.40 | 0.996 | 6.93 |

**Table 3.** Results of the cross-comparisons of different instrumentations on hourly mean data over the full period and during the audit period for $CH_4$. For the full period, the data is filtered for wind speed, however during the audit period no wind speed filtering is applied.

https://doi.org/10.5194/egusphere-2024-3941
Preprint. Discussion started: 8 January 2025


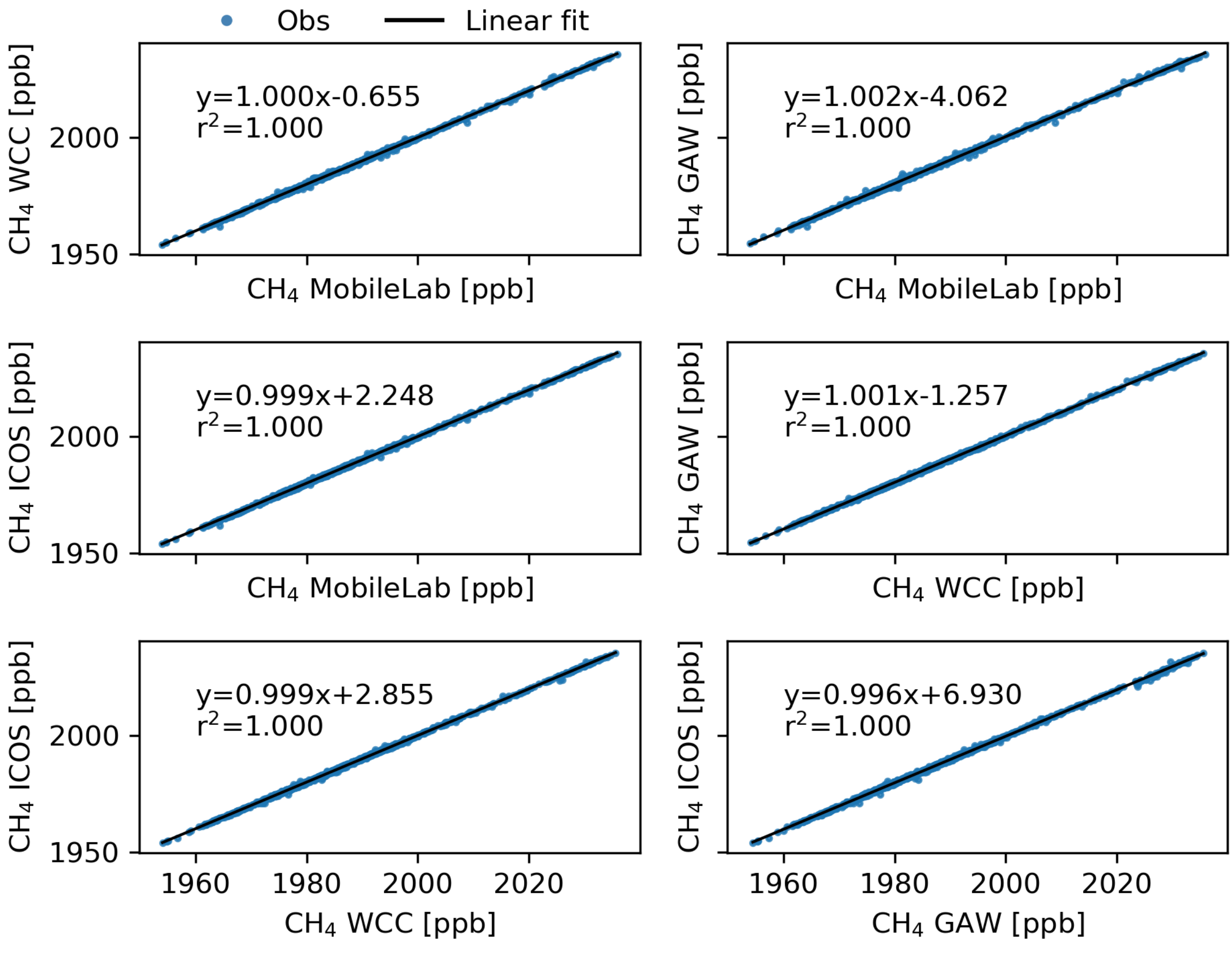


**Figure 14.** Scatterplots and linear regressions fitted to each measurement pair for $CH_4$.

https://doi.org/10.5194/egusphere-2024-3941
Preprint. Discussion started: 8 January 2025


hensive description of the measurement system is presented in Sect. 1, including the used instruments, calibration and target cylinders. The time series of the GAW measurements for $CO_2$ and $CH_4$ are presented with a smoothed and trend curves fitted to the time series. We also present the diurnal and seasonal variations of the de-trended time series. The time series show, as expected, a rise in $CO_2$ and $CH_4$, in agreement with global development. The measured mixing ratios of both $CO_2$ and $CH_4$ at Pallas are higher than the average in the Northern Hemisphere, owing to the station's location in the high latitudes where the greenhouse gas mixing ratios are generally higher than average. The growth rates at Pallas and the average in the northern hemisphere agree in general. However, especially the growth rate of $CH_4$ shows large year-to-year variation, and these variations are more pronounced at Pallas compared to the NOAA MBL. Especially in 2020, the growth rate of $CH_4$ is significantly higher than the average in the northern hemisphere.

The observed differences between the two separate measuring systems at Pallas show a mean difference of less than 0.01 ppm for daily $CO_2$ averages and 0.55 ppb for daily $CH_4$ averages when filtering the measurements to only contain the background signal. An improvement in the agreement between the systems was observed with the addition of Nafion dryer on the intake line of the ICOS instrument. Especially for the $CH_4$ measurements the improvement is clear, the difference before drying the sample is 0.76 ppb on average and 0.21 ppb after. In the $CO_2$ data the effect is less clear, with the difference before adding the Nafion being 0.02 ppm and -0.02 ppm afterward. However, a larger proportion of the data fits within the WMO/GAW compatibility goals after the addition of a dryer, emphasizing the benefit of sample drying. At Pallas, the agreement between the instruments could likely be further improved by drying the sample air of the GAW instrument as well.

Furthermore, the biases observed between the different systems during the ICOS Mobile Laboratory and WCC audits at the station are all shown to be within the WMO/GAW goals. The largest differences were observed between the GAW and WCC systems in both $CO_2$ and $CH_4$, however the largest spread (CI range) in the differences was between ICOS and GAW for $CO_2$ and between GAW and the ICOS Mobile Lab for $CH_4$. This is expected, as the GAW system is the only one measuring from its own inlet and all the other systems are connected to the same inlet. However, even with a slightly different sampling location, the measurements between GAW and the other systems agree well, indicating that the air at Pallas is generally well mixed. Compared to the differences between the ICOS and GAW analyzers over the whole period, the $CO_2$ difference during the audit is slightly higher. This is likely due to the filtering of the data based on the wind speed, assuring well mixed air. However, the spread of the differences over the whole period is slightly larger than only during the audit. For $CH_4$, the mean difference over the entire period is larger compared to the audit period. In addition, the spread was larger. This could be a seasonal effect, as the audit took place in spring when natural $CH_4$ emissions and $CH_4$ and $CO_2$ sinks are lower. Filtering the data by afternoon hours only does not have a large effect on the daily averages when compared to the filtering method based on wind speed and hourly standard deviation. This indicates that the air is generally well mixed during the afternoon hours and that there is little local influence on the mixing ratios.

Our results highlight the good accuracy of the measurements conducted at the Pallas station, as the differences between the two measurement systems are small and fit well within the WMO/GAW network compatibility goals. The audit period also indicates that the ICOS system is performing slightly better, but the effect of theNafion dryer on the differences between the two systems is still unclear. Furthermore, the trend and growth rates at Pallas differ from the NOAA marine boundary layer

https://doi.org/10.5194/egusphere-2024-3941
Preprint. Discussion started: 8 January 2025


trend for the Northern Hemisphere, especially for $CH_4$, demonstrating the importance of atmospheric in-situ observations for detecting regional and local variations in greenhouse gas mixing ratios.

*Data availability.* ICOS $CO_2$ data were downloaded from the ICOS Carbon portal, DOI: 11676/W1KxBw4QLCVKxiEiOVSPoLCU (Hatakka, J. 2024). ICOS $CH_4$ data were downloaded from the ICOS Carbon portal, DOI: 11676/lMY9pSZLevM3UXmNVKiKl4WH (Hatakka, J. 2024). GAW $CO_2$ data were downloaded from the WDCGH, published as CO2_PAL_surface-insitu_FMI_data1 ver. 2024-06-19-0538 at WDCGG (Reference date: 2024/10/15). GAW $CH_4$ data were downloaded from the WDCGH, published as CH4_PAL_surface-insitu_FMI_data1, at WDCGG ver. 2024-06-19-0538 (Reference date: 2024/10/15). The Mobile Laboratory data and GAW audit data are available from the authors on request.

*Author contributions.* AL and HA planned the experiment. AL, HA and JH set up the ICOS Mobile Laboratory audit campaign. CZ and JH set up the GAW audit campaign. HA provided the Mobile Laboratory audit data. CZ provided the GAW audit data. AL analyzed the data. AL prepared the manuscript. AL, HA, CZ, AT, TA and JH contributed to the scientific discussion and preparation of the manuscript.

*Competing interests.* The authors declare that they have no conflict of interest.

*Acknowledgements.* This work has been supported by the The Atmosphere and Climate Competence Centre (IL: Academy of Finland Flagship funding (grant no. 337552, 357904). We thank the ICOS ATC team for the processing of the ICOS instrument data. We would like to thank the ICOS ATC for providing the data on $CO_2$ and $CH_4$.

https://doi.org/10.5194/egusphere-2024-3941
Preprint. Discussion started: 8 January 2025


## References

Crowell, S., Baker, D., Schuh, A., Basu, S., Jacobson, A. R., Chevallier, F., Liu, J., Deng, F., Feng, L., McKain, K., Chatterjee, A., Miller, J. B., Stephens, B. B., Eldering, A., Crisp, D., Schimel, D., Nassar, R., O'Dell, C. W., Oda, T., Sweeney, C., Palmer, P. I., and Jones, D. B. A.: The 2015–2016 carbon cycle as seen from OCO-2 and the global in situ network, Atmospheric Chemistry and Physics, 19, 9797–9831, https://doi.org/10.5194/acp-19-9797-2019, 2019.

Dlugokencky, E. J., Myers, R. C., Lang, P. M., Masarie, K. A., Crotwell, A. M., Thoning, K. W., Hall, B. D., Elkins, J. W., and Steele, L. P.: Conversion of NOAA atmospheric dry air $CH_4$ mole fractions to a gravimetrically prepared standard scale, Journal of Geophysical Research: Atmospheres, 110, 2005JD006 035, https://doi.org/10.1029/2005JD006035, 2005.

Feng, L., Palmer, P. I., Parker, R. J., Lunt, M. F., and Bösch, H.: Methane emissions are predominantly responsible for record-breaking atmospheric methane growth rates in 2020 and 2021, Atmospheric Chemistry and Physics, 23, 4863–4880, https://doi.org/10.5194/acp-23-4863-2023, 2023.

Hall, B. D., Crotwell, A. M., Kitzis, D. R., Mefford, T., Miller, B. R., Schibig, M. F., and Tans, P. P.: Revision of the World Meteorological Organization Global Atmosphere Watch (WMO/GAW) $CO_2$ calibration scale, Atmospheric Measurement Techniques, 14, 3015–3032, https://doi.org/10.5194/amt-14-3015-2021, 2021.

Hammer, S., Konrad, G., Vermeulen, A. T., Laurent, O., Delmotte, M., Jordan, A., Hazan, L., Conil, S., and Levin, I.: Feasibility study of using a "travelling" $CO_2$ and $CH_4$ instrument to validate continuous in situ measurement stations, Atmospheric Measurement Techniques, 6, 1201–1216, https://doi.org/10.5194/amt-6-1201-2013, 2013.

Hatakka, J.: Atmospheric CH4 at Pallas by Finnish Meteorological Institute , dataset published as CH4_PAL_ surface-insitu_FMI_data1 at WDCGG, ver. 2024-06-19-0538 (Reference date: 2024/10/15), 2024a.

Hatakka, J.: Atmospheric CO2 at Pallas by Finnish Meteorological Institute , dataset published as CO2_PAL_ surface-insitu_FMI_data1 at WDCGG, ver. 2024-06-19-0538 (Reference date: 2024/10/15), 2024b.

Hatakka, J.: ICOS ATC CH4 Release, Pallas (12.0 m), 2017-09-16–2024-03-31, https://doi.org/11676/lMY9pSZLevM3UXmNVKiKl4WH, 2024c.

Hatakka, J.: ICOS ATC CO2 Release, Pallas (12.0 m), 2017-09-16–2024-03-31, https://doi.org/11676/W1KxBw4QLCVKxiEiOVSPoLCU, 2024d.

Hatakka, J., Aalto, T., Aaltonen, V., Aurela, M., Hakola, H., Komppula, M., Laurila, T., Lihavainen, H., Paatero, J., Salminen, K., and Viisanen, Y.: Overview of the atmospheric research activities and results at Pallas GAW station, BOREAL ENVIRONMENT RESEARCH, 8, 365–383, 2003.

Hazan, L., Tarniewicz, J., Ramonet, M., Laurent, O., and Abbaris, A.: Automatic processing of atmospheric $CO_2$ and $CH_4$ mole fractions at the ICOS Atmosphere Thematic Centre, Atmospheric Measurement Techniques, 9, 4719–4736, https://doi.org/10.5194/amt-9-4719-2016, 2016.

Heiskanen, J., Brümmer, C., Buchmann, N., Calfapietra, C., Chen, H., Gielen, B., Gkritzalis, T., Hammer, S., Hartman, S., Herbst, M., Janssens, I. A., Jordan, A., Juurola, E., Karstens, U., Kasurinen, V., Kruijt, B., Lankreijer, H., Levin, I., Linderson, M.-L., Loustau, D., Merbold, L., Myhre, C. L., Papale, D., Pavelka, M., Pilegaard, K., Ramonet, M., Rebmann, C., Rinne, J., Rivier, L., Saltikoff, E., Sanders, R., Steinbacher, M., Steinhoff, T., Watson, A., Vermeulen, A. T., Vesala, T., Vítková, G., and Kutsch, W.: The Integrated Carbon Observation System in Europe, Bulletin of the American Meteorological Society, 103, E855–E872, https://doi.org/10.1175/BAMS-D-19-0364.1, 2022.

Lan, X., Tans, P., and Thoning, K.: Trends in globally-averaged CO2 determined from NOAA Global Monitoring Laboratory measurements. Version 2024-04, https://doi.org/10.15138/9N0H-ZH07, 2024a.

Lan, X., Thoning, K., and Dlugokencky, E.: Trends in globally-averaged CH4, N2O, and SF6 determined from NOAA Global Monitoring Laboratory measurements. Version 2024-04, https://doi.org/10.15138/P8XG-AA10, 2024b.

Levin, I., Karstens, U., Eritt, M., Maier, F., Arnold, S., Rzesanke, D., Hammer, S., Ramonet, M., Vítková, G., Conil, S., Heliasz, M., Kubistin, D., and Lindauer, M.: A dedicated flask sampling strategy developed for Integrated Carbon Observation System (ICOS) stations based on $CO_2$ and CO measurements and Stochastic Time-Inverted Lagrangian Transport (STILT) footprint modelling, Atmospheric Chemistry and Physics, 20, 11 161–11 180, https://doi.org/10.5194/acp-20-11161-2020, 2020.

Nisbet, E. G., Dlugokencky, E. J., Manning, M. R., Lowry, D., Fisher, R. E., France, J. L., Michel, S. E., Miller, J. B., White, J. W. C., Vaughn, B., Bousquet, P., Pyle, J. A., Warwick, N. J., Cain, M., Brownlow, R., Zazzeri, G., Lanoisellé, M., Manning, A. C., Gloor, E., Worthy, D. E. J., Brunke, E.-G., Labuschagne, C., Wolff, E. W., and Ganesan, A. L.: Rising atmospheric methane: 2007-2014 growth and isotopic shift: RISING METHANE 2007-2014, Global Biogeochemical Cycles, 30, 1356–1370, https://doi.org/10.1002/2016GB005406, 2016.

Nisbet, E. G., Manning, M. R., Dlugokencky, E. J., Fisher, R. E., Lowry, D., Michel, S. E., Myhre, C. L., Platt, S. M., Allen, G., Bousquet, P., Brownlow, R., Cain, M., France, J. L., Hermansen, O., Hossaini, R., Jones, A. E., Levin, I., Manning, A. C., Myhre, G., Pyle, J. A., Vaughn, B. H., Warwick, N. J., and White, J. W. C.: Very Strong Atmospheric Methane Growth in the 4 Years 2014–2017: Implications for the Paris Agreement, Global Biogeochemical Cycles, 33, 318–342, https://doi.org/10.1029/2018GB006009, 2019.

Peiro, H., Crowell, S., Schuh, A., Baker, D. F., O'Dell, C., Jacobson, A. R., Chevallier, F., Liu, J., Eldering, A., Crisp, D., Deng, F., Weir, B., Basu, S., Johnson, M. S., Philip, S., and Baker, I.: Four years of global carbon cycle observed from the Orbiting Carbon Observatory 2 (OCO-2) version 9 and in situ data and comparison to OCO-2 version 7, Atmospheric Chemistry and Physics, 22, 1097–1130, https://doi.org/10.5194/acp-22-1097-2022, 2022.

Peng, S., Lin, X., Thompson, R. L., Xi, Y., Liu, G., Hauglustaine, D., Lan, X., Poulter, B., Ramonet, M., Saunois, M., Yin, Y., Zhang, Z., Zheng, B., and Ciais, P.: Wetland emission and atmospheric sink changes explain methane growth in 2020, Nature, 612, 477–482, https://doi.org/10.1038/s41586-022-05447-w, 2022.

Qu, Z., Jacob, D. J., Zhang, Y., Shen, L., Varon, D. J., Lu, X., Scarpelli, T., Bloom, A., Worden, J., and Parker, R. J.: Attribution of the 2020 surge in atmospheric methane by inverse analysis of GOSAT observations, Environmental Research Letters, 17, 094 003, https://doi.org/10.1088/1748-9326/ac8754, 2022.

Rella, C. W., Chen, H., Andrews, A. E., Filges, A., Gerbig, C., Hatakka, J., Karion, A., Miles, N. L., Richardson, S. J., Steinbacher, M., Sweeney, C., Wastine, B., and Zellweger, C.: High accuracy measurements of dry mole fractions of carbon dioxide and methane in humid air, Atmospheric Measurement Techniques, 6, 837–860, https://doi.org/10.5194/amt-6-837-2013, 2013.

Resovsky, A., Ramonet, M., Rivier, L., Tarniewicz, J., Ciais, P., Steinbacher, M., Mammarella, I., Mölder, M., Heliasz, M., Kubistin, D., Lindauer, M., Müller-Williams, J., Conil, S., and Engelen, R.: An algorithm to detect non-background signals in greenhouse gas time series from European tall tower and mountain stations, Atmospheric Measurement Techniques, 14, 6119–6135, https://doi.org/10.5194/amt-14-6119-2021, 2021.

Stevenson, D. S., Derwent, R. G., Wild, O., and Collins, W. J.: COVID-19 lockdown emission reductions have the potential to explain over half of the coincident increase in global atmospheric methane, Atmospheric Chemistry and Physics, 22, 14 243–14 252, https://doi.org/10.5194/acp-22-14243-2022, 2022.

https://doi.org/10.5194/egusphere-2024-3941
Preprint. Discussion started: 8 January 2025


Tenkanen, M. K., Tsuruta, A., Denier Van Der Gon, H., Höglund-Isaksson, L., Leppänen, A., Markkanen, T., Petrescu, A. M. R., Raivonen, M., and Aalto, T.: Partitioning anthropogenic and natural methane emissions in Finland during 2000–2021 by combining bottom-up and top-down estimates, https://doi.org/10.5194/egusphere-2024-1953, 2024.

Thonat, T., Saunois, M., Bousquet, P., Pison, I., Tan, Z., Zhuang, Q., Crill, P. M., Thornton, B. F., Bastviken, D., Dlugokencky, E. J., Zimov, N., Laurila, T., Hatakka, J., Hermansen, O., and Worthy, D. E. J.: Detectability of Arctic methane sources at six sites performing continuous atmospheric measurements, Atmospheric Chemistry and Physics, 17, 8371–8394, https://doi.org/10.5194/acp-17-8371-2017, 2017.

Thoning, K. W., Tans, P. P., and Komhyr, W. D.: Atmospheric carbon dioxide at Mauna Loa Observatory: 2. Analysis of the NOAA GMCC data, 1974-1985, Journal of Geophysical Research: Atmospheres, 94, 8549–8565, https://doi.org/10.1029/JD094iD06p08549, 1989.

Vardag, S. N., Hammer, S., O'Doherty, S., Spain, T. G., Wastine, B., Jordan, A., and Levin, I.: Comparisons of continuous atmospheric $CH_4$, $CO_2$ and $N_2O$ measurements – results from a travelling instrument campaign at Mace Head, Atmospheric Chemistry and Physics, 14, 8403–8418, https://doi.org/10.5194/acp-14-8403-2014, 2014.

Ward, R. H., Sweeney, C., Miller, J. B., Goeckede, M., Laurila, T., Hatakka, J., Ivakov, V., Sasakawa, M., Machida, T., Morimoto, S., Goto, D., and Ganesan, A. L.: Increasing Methane Emissions and Widespread Cold-Season Release From High-Arctic Regions Detected Through Atmospheric Measurements, Journal of Geophysical Research: Atmospheres, 129, e2024JD040 766, https://doi.org/10.1029/2024JD040766, 2024.

WMO: 16th WMO/IAEA Meeting on Carbon Dioxide, Other Greenhouse Gases, and Related Measurement Techniques (GGMT-2011), Tech. Rep. 206, WMO, Wellington, https://library.wmo.int/idurl/4/51479, 2013.

WMO: System and Performance Audit of Surface Ozone, Carbon Monoxide, Methane, Carbon Dioxide and Nitrous Oxide at the Global GAW Station Pallas, Finland, July 2021, Tech. Rep. 283, WMO, Geneva, https://library.wmo.int/idurl/4/66280, 2022.

WMO: Twenty-First WMO/IAEA Meeting on Carbon Dioxide, Other Greenhouse Gases and Related Measurement Techniques (GGMT-2022), Tech. Rep. 292, WMO, Geneva, https://library.wmo.int/idurl/4/68925, 2024.

Yuan, K., Li, F., McNicol, G., Chen, M., Hoyt, A., Knox, S., Riley, W. J., Jackson, R., and Zhu, Q.: Boreal–Arctic wetland methane emissions modulated by warming and vegetation activity, Nature Climate Change, 14, 282–288, https://doi.org/10.1038/s41558-024-01933-3, 2024.

Zellweger, C., Emmenegger, L., Firdaus, M., Hatakka, J., Heimann, M., Kozlova, E., Spain, T. G., Steinbacher, M., Van Der Schoot, M. V., and Buchmann, B.: Assessment of recent advances in measurement techniques for atmospheric carbon dioxide and methane observations, Atmospheric Measurement Techniques, 9, 4737–4757, https://doi.org/10.5194/amt-9-4737-2016, 2016.

Zellweger, C., Steinbrecher, R., Laurent, O., Lee, H., Kim, S., Emmenegger, L., Steinbacher, M., and Buchmann, B.: Recent advances in measurement techniques for atmospheric carbon monoxide and nitrous oxide observations, Atmospheric Measurement Techniques, 12, 5863–5878, https://doi.org/10.5194/amt-12-5863-2019, 2019.

Zhou, L., Kitzis, D., Tans, P., Masarie, K., and Chao, D.: WMO Round-Robin Inter-comparison: Progress and a New Website, in: 15th WMO/IAEA Meeting of Experts on Carbon Dioxide, Other Greenhouse Gases and Related Tracers Measurement Techniques, no. 194 in GAW Report, pp. 161–164, WMO, Jena, https://library.wmo.int/idurl/4/58718, 2009.